View metadata, citation and similar papers at core.ac.uk

brought to you by CORE

provided by LSHTM Research Online

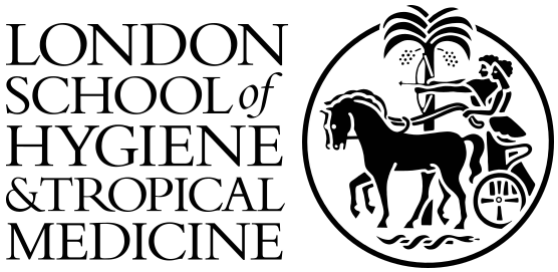

LSHTM Research Online

Collorone, Sara; Prados, Ferran; Hagens, Marloes HJ; Tur, Carmen; Kanber, Baris; Sudre, Carole H; Lukas, Carsten; Gasperini, Claudio; Oreja-Guevara, Celia; Andelova, Micaela; +7 more... Ciccarelli, Olga; Wattjes, Mike P; Ourselin, Sebastian; Altmann, Daniel R; Tijms, Betty M; Barkhof, Frederik; Toosy, Ahmed T; (2019) Single-subject structural cortical networks in clinically isolated syndrome. Multiple Sclerosis Journal. p. 135245851986573. ISSN 1352-4585 DOI: https://doi.org/10.1177/1352458519865739

Downloaded from: http://researchonline.lshtm.ac.uk/4653799/

DOI: https://doi.org/10.1177/1352458519865739

**Usage Guidelines:**

Please refer to usage guidelines at https://researchonline.lshtm.ac.uk/policies.html or alternatively contact researchonline@lshtm.ac.uk.

Available under license: http://creativecommons.org/licenses/by-nc-nd/2.5/

https://researchonline.lshtm.ac.uk

**Title:** Single-Subject Structural Cortical Networks in Clinically Isolated Syndrome.

**Authors:** Sara Collorone[1], MD; Ferran Prados [1,2,3], PhD; Marloes H.J. Hagens[4], PhD; Carmen Tur [1], PhD; Baris Kanber[2], PhD; Carole H. Sudre[5], PhD; Carsten Lukas[6], PhD; Claudio Gasperini[7], PhD; Celia Oreja-Guevara[8], PhD; Micaela Andelova[9,10], PhD; Olga Ciccarelli [1,11], PhD; Mike P. Wattjes[12,13], PhD; Sebastian Ourselin[5,14], PhD; Daniel R. Altmann[15], PhD; Betty M. Tijms[16], PhD; Frederik Barkhof [2,11,16,17], PhD; Ahmed T. Toosy[1], PhD; for the MAGNIMS Study Group

1 NMR Research Unit, Queen Square MS Centre, Department of Neuroinflammation, UCL Institute of Neurology, Faculty of Brain Sciences, UCL, London, United Kingdom

2 Centre for Medical Image Computing (CMIC), Department of Medical Physics and Biomedical Engineering, UCL, London, United Kingdom

3. Universitat Oberta de Catalunya, Barcelona, Spain

4. MS Center Amsterdam, Department of Neurology, Amsterdam UMC, Vrije Universiteit Amsterdam, Amsterdam, The Netherlands

5. Department of Medical Physics and Biomedical Engineering, UCL, London, United Kingdom

6. Department of Diagnostic and Interventional Radiology and Nuclear Medicine, St. Josef Hospital, Ruhr University, Bochum, Germany

7. Department of Neurosciences, San Camillo-Forlanini Hospital, Rome, Italy

8. Department of Neurology, Hospital Clinico San Carlos, Instituto de Investigacion Sanitaria del Hospital Clınico San Carlos (IdISSC), Madrid, Spain

9. Neurologic Clinic and Policlinic, University Hospital Basel, University of Basel, Basel, Switzerland

10. Charles University and General Hospital, Prague, Czech Republic

11. NIHR University College London Hospitals Biomedical Research Centre, London, United Kingdom

12. MS Center Amsterdam, Department of Radiology and Nuclear Medicine, Amsterdam UMC, Vrije Universiteit Amsterdam, Amsterdam, The Netherlands

13. Department Of Diagnostic and Interventional Neuroradiology, Hannover Medical School, Hannover, Germany

14. Department of Imaging and Biomedical Engineering, King's College London, London, United Kingdom

15. London School of Hygiene and Tropical Medicine, London, United Kingdom

16. Alzheimer Center and Department of Neurology, Amsterdam University Medical Centers, Amsterdam Neuroscience, Vrije Universiteit Amsterdam, Amsterdam, the Netherlands.

17. Institutes of Neurology & Healthcare Engineering, UCL Institute of Neurology, UCL, London, United Kingdom

**Correspondent author:**

Dr. Sara Collorone

Queen Square Multiple Sclerosis Centre

Department of Neuroinflammation, UCL Institute of Neurology

1st Floor, Russell Square House, 10-12 Russell Square

London

WC1B 5EH

e-mail: s.collorone@ucl.ac.uk

Twitter: @SaraCollorone

Tel.: +44 (0) 7400254777

**Keywords:** magnetic resonance imaging; multiple sclerosis; clinically isolated syndrome; gray matter; graph theory; structural cortical networks; multicenter study

**ABSTRACT**

Background: Structural cortical networks (SCNs) represent patterns of coordinated morphological modifications in cortical areas and they present the advantage of being extracted from previously acquired clinical MRI scans. SCNs have shown pathophysiological changes in many brain disorders, including multiple sclerosis.

Objective: To investigate alterations of SCNs at the individual level in patients with clinically isolated syndrome (CIS), thereby assessing their clinical relevance.

Methods: We analyzed baseline data collected in a prospective multi-center (MAGNIMS) study. CIS patients (n=60) and healthy controls (n=38) underwent high resolution 3T MRI. Measures of disability and cognitive processing were obtained for patients. Single-subject structural cortical networks were extracted from brain 3D-T1 weighted sequences; global and local network parameters were computed.

Results: Compared to healthy controls, CIS patients showed altered small-world topology, an efficient network organization combining dense local clustering with relatively few long-distance connections. These disruptions were worse for patients with higher lesion load and worse cognitive processing speed. Alterations of centrality measures and clustering of connections were observed in specific cortical areas in CIS patients when compared with healthy controls.

Conclusion: Our study indicates that SCNs can be used to demonstrate clinically relevant alterations of connectivity in clinically isolated syndrome.

## INTRODUCTION

Multiple sclerosis (MS) is a chronic inflammatory demyelinating and degenerative disease of the central nervous system. For most patients, MS starts with an acute neurological episode known as a clinically isolated syndrome (CIS)[1]. Conventional MRI findings are the best predictors of conversion to MS, although measures such as the WM lesion volume only partially correlate with the variable course of the disease[2]. MRI abnormalities in the normal-appearing white and gray matter, and connectivity alterations may contribute to clinical outcome of patients with CIS[3]. Functional changes in the brain can lead to related morphological modification in cortical areas[4,5] and, recently, it has become possible to describe these coordinated patterns of cortical morphology with network parameters[6]. In structural cortical networks (SCNs), the nodes correspond to cortical areas considered connected by edges when they have structural similarity in thickness or volume across subjects[7] or within single subjects[8]. In comparison with other brain graphs (e.g., structural graphs derived from diffusion tensor imaging or functional graphs derived from synchronic activation of brain areas), SCNs present the unique advantage of being derived from anatomical MRI acquisitions, such as a 3D T1-weighted sequence, frequently available in acquired datasets and even in routine clinical protocols.

SCNs have shown clinically relevant changes in many brain diseases[9–11]. However, few studies so far have investigated SCNs in multiple sclerosis (MS)[12–15].

SCN analysis has revealed in MS patients a disruption of physiological small-world network topology of the brain: an efficient organization, shared by most of the complex systems in nature, including brain networks, that is neither completely regular nor completely random, because it combines a dense local clustering with relatively few long-distance connections[16]. Whilst MS patients can shift in either direction, either a more regular[13,14] or a more random network[12,15], the only study including a small cohort of CIS patients[14] demonstrated an increased clustered organization of SCNs in CIS subjects compared with healthy controls (HCs). Regular networks, such as lattices, are highly clustered, but with a long path length: nodes are densely connected with

their clique of neighbors, whereas they are linked to distant nodes only through several intermediate steps, causing a decrease in the global network efficiency. However, the SCNs were extracted at group level in the CIS cohort, and so it remains unclear whether and how these disruptions are associated with individual measures of disability.

Our aim was to investigate SCNs alterations in a larger CIS patient cohort by constructing the network at the individual level, thereby assessing the clinical relevance of the SCN alterations. Moreover, since SCNs have been studied exclusively in single-center studies before, our secondary aim was to evaluate the impact of across-scanner variations on single-subject SCNs analysis.

## MATERIALS AND METHODS

### *Participants*

This study represents a re-analysis of the baseline data which were acquired as part of a prospective MAGNIMS (www.magnims.eu) 3-year multi-center, multi-vendor project, conducted at the following six MS Centers (Table 1). Previous studies using the same cohort addressed a different issue and are unrelated to this analysis[17,18].

Sixty patients experiencing symptoms suggestive of a CIS (age 18 to 59 years at baseline) were recruited from the six participating centers within six months of symptom onset. Thirty-eight age and gender-matched healthy controls (HCs) were also recruited (Table 1). Exclusion criteria for all participants were a history of other known medical conditions that could have affected the brain (vascular, malignant, neurological) and MRI related contra-indications.

### *Clinical examination*

At baseline, CIS patients underwent neurological examination and Expanded Disability Status Scale (EDSS) was assessed by a trained physician. Forty-seven patients were also tested for information processing speed with the Symbol Digit Modality Test (SDMT).

### *Image acquisition and post-processing*

All subjects underwent a baseline MRI scan of the brain and spinal cord at a 3T scanner, and CIS patients additionally underwent administration of intravenous contrast. The scanning parameters were based on local protocols and followed the MAGNIMS guidelines[19]. The acquisition protocols for the different vendors has been previously described[18]: it included brain 3D T1-weighted (1mm isotropic) and 3D fluid-attenuated inversion recovery (FLAIR); proton density/T2 and post-contrast T1-weighted sequences for brain and spinal cord.

White matter lesion number and location (periventricular, juxtacortical, deep WM, infratentorial and spinal) were recorded. Subsequently, dissemination in space and time, as well as MS diagnosis, were determined according to the revised 2017 McDonald criteria[20].

White matter lesion segmentation was performed with a semi-automated process using the 3D FLAIR and 3D T1-weighted MRI sequences[21] All lesion masks were checked, corrected manually and lesion volumes subsequently obtained. These lesion masks were registered to the 3D T1-weighted sequence and the registered T1 lesion masks were used for lesion filling[22], after which cortical gray matter (CGM) was automatically segmented and parcellated using GIF[23]. All segmentations were quality checked. Ninety-eight cortical areas were identified in the native-space bilateral CGM according to the Desikan-Killiany-Tourville protocol (http://braincolor.mindboggle.info)[24].

For computational reasons, CGM segmentation on the 3D T1-weighted images was resliced to 2.0 mm isotropic voxels to reduce the dimensionality of the data[8].

***Single-subject gray matter graphs***

SCNs were extracted at subject level using software developed by T.B.M (https://github.com/bettytijms/Single_Subject_Grey_Matter_Networks) in Matlab v7.12.0.635. Briefly, first, the SCNs' nodes were defined as regions-of-interest in the native space CGM segmentation, corresponding to 3x3x3 voxel cubes. This was chosen because a 3-voxel size can capture the thickness and folding of the cortex[25] without generating large matrices of cubes.

The similarity between all the cubes (nodes) in the network was determined with the correlation coefficient, which was collected in a matrix that was subsequently thresholded and binarized, so that the chance of having spurious correlations for all single-subject SCNs was < or = to 5%. The obtained graphs were undirected with nodes connected each other by edges, only if their similarity matrix survived this threshold (Figure 1).

***Graph properties***

First, we determined the following global graph-defining properties: the size of the SCNs (i.e., the number of cubes), the average degree (i.e., the number of edges) and the connectivity density (i.e., the proportion of existing connections to the maximum number of possible connections). Then, we computed the global graph parameters averaged across all cubes: the characteristic path length[26], the clustering coefficient[16], the betweenness centrality[27] and the eigenvector centrality[28]. In addition, the clustering coefficient and characteristic path length of each graph were normalised with those of 20 randomised reference graphs of identical size and degree distribution[8]. The small-world coefficient was then obtained from the ratio between the normalised clustering coefficient ($\gamma$) and the normalised characteristic path length ($\lambda$). A network shows a small-world properties when its nodes are highly clustered, as in regular lattices, but they can also be reached from every other node in a small number of steps, e.g. in random graphs, resulting in a ratio between $\gamma$ and $\lambda$ greater than 1[29].

At regional level, we averaged the local graph parameters across the nodes within each of the 98 cortical areas, which had been parcellated with GIF in each individual subject, in order to reduce the dimensionality of the SCNs and increase the comparability between subjects, across centers and possibly with previous studies[30].

***Statistical analysis***

Group differences in demographic characteristics and CGM volume were assessed using two-sample t-tests for continuous variables and chi-square tests for categorical variables.

We initially applied a multivariate linear regression model to compare graph properties between groups adjusting for age and gender and CGM volume. Since non-normalised global graph parameters (betweenness centrality, eigenvector centrality, clustering coefficient and path length) are dependent on graph-defining properties (size, connectivity density and degree), we included any of these graph-defining properties when they were significantly different between groups as additional independent variables to the model. We tested possible nonlinear effects of age with quadratic regression analysis imputing graph parameters as dependent variables.

Since the analysis of the global graph parameters was meant to be exploratory, we did not perform multiple comparison adjustments.

Group differences in local graph parameters in the 98 CGM areas were assessed with linear regression, correcting for age, gender and local CGM volume). Due to concerns about residual variance heterogeneity across centers, the regression was estimated using the Hubert-White[31,32] standard error, which is known to be robust to residual heterogeneity. Significant P values were identified correcting for multiple comparisons using a False Discovery Rate (FDR) of 5% for multiple hypothesis testing[33].

WM lesion volumes were log transformed to allow parametric testing[34] and the relationships between these and global/local graph metrics as well as clinical parameters (EDSS, SDMT, MS diagnosis according to the 2017 McDonald criteria) were assessed using linear regression adjusting for age and gender. Associations between local/global graph metrics changes and clinical parameters were assessed with linear regression adjusting for age and gender. The WM lesion volume was included as an additional independent variable to the model if associated with the clinical parameters.

Since CIS patients are heterogeneous in terms of the number of WM lesions, an established risk factor for conversion to MS, we also divided patients into distinct groups according to the number of intracranial WM lesions: 0-1, 2-9 and >10 lesions (Table 1). This allowed further comparisons between HCs and patients at different risk stage of developing MS[35].

Not all centers provided both HCs and patients, hence we investigated and controlled for center effects in the following manner. In addition to entering the center as a covariate in a linear regression including all centers, with graph metrics as dependent variables and age, gender and CGM volume as the other covariates, we performed a further analysis restricted to those centers contributing both patients and HCs (Basel, Bochum and London). If the between-group graph parameter differences or p-values were materially altered by inclusion of center in either the full or the restricted analyses, center was retained as covariate in the unrestricted model over all centers. Statistical analyses were performed with Stata v. 14.1 (Stata Corporation, College Station, Texas, USA).

## RESULTS

### Subject Characteristics

The clinical and radiological characteristics of the participants (60 patients and 38 healthy controls) are provided in Table 1. CIS patients and HCs did not show significant differences in age, gender and CGM volumes. CIS patients had low disability and were cognitively preserved. Out of the entire sample of 60 patients, eight fulfilled the 2017 McDonald criteria for MS.

Participants' characteristics across centers are detailed in eTable1 in Supporting Information.

### Global graph metrics

All single-subject SCNs did not exhibit disconnected nodes.

Both CIS and HC groups retained small-world topology ($\gamma/\lambda>1$), but in CIS patients the multivariate regression analysis ($R^2=0.06$, $F(4, 92)=2.38$, $p<0.05$) showed a higher $\gamma$ than HCs (B= 0.01, 95% CIs=0.003-0.02, p=0.012) . CIS patients showed also ($R^2=0.11$, $F(4, 92)=3.41$, $p<0.05$) a higher small-world coefficient than HCs (B= 0.01, 95% CIs=0.004-0.02, p=0.003).

Age and age squared did not have any effects on the global graph metrics.

After correction for center effect, the differences between CIS patients and HCs for small-world coefficient remained significant (p=0.024) but not for $\gamma$ (Table 2).

Center/scanner effect was also significant for connectivity density ($p<0.0001$) and for all global graph parameters ($p<0.0001$). Therefore, center was retained as covariate in the multivariate regression analysis. See eTable2 in Supplemental Material for the SCNs parameters across centers. For global graph-defining properties, CIS patients had smaller network sizes compared with HCs (Table 2); therefore, in order to compare SCNs between CIS and HC groups, we adjusted the analysis of the non-normalised global graph parameters for the network size. CIS patients initially showed higher eigenvector centrality than controls (B=0.07, 95% CIs=0.01-0.1, p=0.02), but this difference lost significance after adjusting for network size (Table 2).

In CIS patients, a higher small-world coefficient was associated ($R^2=0.17$, $F(3, 55)=3.64$, $p<0.05$) with higher WM lesion volume ($\beta= 0.36$, $p=0.007$), after adjusting for age ($\beta= 0.03$, $p=0.832$) and gender ($\beta= -0.18$, $p=0.162$); additionally, CIS patients with higher lesion counts (>10 lesions) showed higher gamma and greater small-world coefficients compared with HCs and with CIS patients with lower lesion numbers (Figure 2). The small-world coefficient in CIS patients and the WM lesion location were not significantly associated.

Amongst the 47 CIS patients with SDMT scores available, a higher small-world coefficient was associated ($R^2=0.21$,$F(3,43)=3.86$, $p<0.05$) with a lower SDMT score (i.e. slower information processing speed) ($\beta= -0.39$, $p=0.008$) after adjusting for age ($\beta= -0.81$, $p=0.42$) and gender ($\beta= 0.85$, $p=0.4$) (Figure 3). There were too few MS patients (n=9) in our cohort to allow comparisons with HCs and other CIS patients not diagnosed with MS.

**Local graph metrics**

We investigated whether differences between CIS patients and HCs were specific to particular cortical areas. Patients and controls showed similar volumes in the 98 CGM areas and there were no significant differences in degree. Several cortical areas showed significant differences for betweenness centrality, clustering coefficient and path length ($p<0.05$), but only three survived correction for multiple testing (see eTable3 in Supplemental Material). Patients showed lower betweenness centrality in the right superior frontal gyrus ($0.30\pm0.01$ vs $0.33\pm0.01$, $p<0.0001$;

$p_{FDR}$<0.05) and lower clustering coefficient in the right postcentral gyrus (0.51±0.04 vs 0.54±0.03, p<0.0001; $p_{FDR}$<0.05) in comparison to HCs (Figure 4). Among CIS patients, these alterations were not correlated with clinical parameters or WM lesion volume.

Finally, CIS patients with >10 WM lesions had lower betweenness centrality in the right postcentral gyrus (0.29±0.01 0.33±0.01, $p_{FDR}$<0.05) and lower clustering coefficient in the right medial orbital gyrus (0.51±0.04 vs 0.53±0.03, $p_{FDR}$<0.05), compared with HCs.

There was significant ($p_{FDR}$<0.05) variability across centers in the following local graph properties: characteristic path length in the bilateral anterior insula, left inferior and middle temporal gyrus, left parahippocampal gyrus; clustering coefficient in the right inferior and middle occipital gyrus; betweenness centrality in the left posterior cingulate cortex and eigenvector centrality in the right middle occipital gyrus.

**DISCUSSION**

In this study, using single-subject SCN analysis, we showed that in CIS patients, graph alterations are related to disease burden. At the global level, CIS patients possess altered small-world topology characterized by a shift towards a more regular network. These findings are in line with previous studies on SCNs in CIS patients[14]. A regular network tends to possess dense local connections (i.e. high clustering) between nodes at the expenses of the long-distance ones (i.e. low path length), thus compromising the efficient balance between short and long-range information transfer, distinctive of small-world networks[16].

When comparing the whole CIS cohort with HCs, the difference in small-world coefficient was significant, but small. This small difference could be because CIS patients were at the very onset of the disease, some of them with little WM damage. When patients were stratified according to the number of WM lesions, this difference in the small-world coefficient increased: subjects with higher lesion load at onset showed higher small-world coefficient values compared not only with HCs, but also with the group of CIS patients with 0-1 lesion.

This altered topology was correlated with a high lesion load. Moreover, we did not find any significant differences in cortical volumes between groups: in CIS patients the tendency to lose long-distance connections could be a consequence of altered connectivity due to lesional disruption of WM tracts more than to alterations in cortical areas.

The increase in the small-world coefficient, in our study, was associated with worse cognitive performance. Noteworthy, the analysis of single-subject SCNs in established MS[15], similar to studies conducted with the same methodology in dementia[10], showed that cognitively impaired patients tend to possess random SCN topology. However, unlike individuals in our cohort, those patients already had evidence of definite gray matter atrophy. This suggests that small-world topology alterations of the SCNs may have different characteristics at different stages of the disease, being more regular in the early phases and more random when neurodegeneration starts to occur.

At local level, CIS patients had altered network properties in several cortical region, including low clustering coefficient in areas relevant to cognition. These alterations do not seem to affect the global SCNs properties and the clinical phenotype. However, studies with further cognitive assessments and longitudinal follow-up could investigate the clinical relevance of these findings.

In our study, SCNs differed in size between CIS patients and HCs, although the two groups did not show any difference in CGM volume. It is possible that the smaller size of patients' SCNs could result from the different MRI pre-processing, particularly the WM lesion segmentation in patients, or from the presence of intra-cortical lesions. Most studies use methods that constrain networks into identical sizes (i.e. parcellated cortical areas), whereas, here, we chose to extract SCNs from native space segmentations, thus preserving the inter-individual variability. However, it is still not clear how to compare graphs with different sizes and/or connectivity densities[30]. Here, we adjusted for SCN size in our statistical models, but after this, we could not detect any differences in non-normalised global graph-parameters between CIS patients and HCs.

One final consideration is the multi-center setting of our study giving rise to inter-center variability. Inter-scanner variations had significant effects on the global graph parameters. This may have been due to differences in WM-GM interface contrast across different scanners that influenced the CGM segmentation outcomes. Our findings suggest that it is important to account for inter-center variability for single-subject SCN extraction from multi-center neuroimaging datasets. The advantage of multi-center settings though is the putative increase in statistical power and, although variance heterogeneity across centers may be a potential problem for our analysis, the relative robustness of the small-world result suggests this may not in our case be a major limitation.

## CONCLUSIONS

In this study, we applied, for the first time, a recently developed method to extract single-subject SCNs in CIS. Using clinical scans, we were able to demonstrate altered small-world topology in CIS patients SCNs that was associated with cognitive processing. This suggests that SCNs are affected early in MS and can represent a potential biomarker. Future longitudinal analyses will assess if the observed changes in SCNs can predict conversion to MS during the follow-up.

**ACKNOWLEDGMENTS**

This research study was supported by ECTRIMS-MAGNIMS fellowship program, Rosetrees Trust and by the National Institute for Health Research University College London Hospitals Biomedical Research Centre. The part of the study from Bochum was supported by the German Federal Ministry for Education and Research, BMBF, German Competence Network Multiple Sclerosis (KKNMS), grant no. 01GI1601I and grant no. 01GI0914.

The authors thank the collaborators from the MAGNIMS centers involved in this study. For the Basel center, Michael Amann contributed to the MAGNIMS data set used in this study in collaboration with Johanna Lieb and under the supervision of Till Sprenger and Ludwig Kappos. For the London center, Niamh Cawley contributed to the MAGNIMS data set used in this study. For the Bochum center, the authors wish to acknowledge the work of Dr. Barabara Bellenberg. For the Amsterdam center, the authors wish to acknowledge the work of Joep Killestein, Jessica Burggraaff and Iris Kilsdonk.

The authors thank the following MAGNIMS steering committee members for their contribution to the study design: Tarek Yousry, MD, PhD (Queen Square MS Centre, UCL Institute of Neurology); Nicola De Stefano, MD, PhD (University of Siena); Christian Enzinger, MD, PhD (Medical University of Graz); Massimo Filippi, MD, PhD (San Raffaele Scientific Institute, VitaSalute San Raffaele University); Maria A. Rocca (San Raffaele Scientific Institute, Vita-Salute San Raffaele University); Jette L. Frederiksen, MD, PhD (Glostrup Hospital and University of Copenhagen); Ludwig Kappos, MD, PhD (University of Basel); Jacqueline Palace, MD, PhD (University of Oxford Hospitals Trust); Alex Rovira, MD, PhD (Hospital Universitari Vall d'Hebron, Universitat Aut`onoma de Barcelona); Jauma Sastre-Garriga, MD, PhD (Hospital Universitari Vall d'Hebron, Universitat Autonoma de Barcelona); Hugo Vrenken, MD, PhD (MS Centre VU University Medical Centre Amsterdam).

## CONFLICT OF INTEREST STATEMENT

**SC** received an ECTRIMS-MAGNIMS fellowship in 2016 and receives funding from Rosetrees Trust. **FP** is a non-clinical Guarantors of the Brain fellow. He has also received honoraria from Bioclinica Inc. **CT** has received a post-doctoral research ECTRIMS fellowship (2015); she is a consultant for F. Hoffmann-La Roche Ltd and has received honoraria and support for travelling from Novartis, F. Hoffmann-La Roche Ltd, Teva Pharmaceuticals and Ismar Healthcare. **CL** holds an endowed professorship supported by the Novartis Foundation, has received consulting and speaker's honoraria from Biogen-Idec, Bayer Schering, Novartis, Sanofi, Genzyme, and TEVA, and has received research scientific grant support from Merck-Serono and Novartis. **CG** is a member of the Scientific Advisory Boards of Merck, Genzyme, Teva and Biogen; he has received funding for travel or speaker honoraria from Merck, Genzyme, Biogen, Teva Novartis and Roche. **CO-G** received honoraria as speaker from BiogenIdec, Roche, Merck-Serono, Teva, Genzyme, and Novartis. **MA** has received travel and conference fees support from Novartis and Biogen. **OC** is a member of the Scientific Advisory Boards of Teva, Novartis, Roche, Biogen and Merck; she has received funding for travel or speaker honoraria from Teva, Novartis, Roche, Biogen and Merck; she is Associate Editor of Neurology and she serves on the Editorial Board of Multiple Sclerosis Journal; she receives research support from the NIHR UCLH/UCL Biomedical Research Centre, NIHR, MS Society of Great Britain and Northern Ireland, National MS Society, Rosetrees Trust. **MPW** serves as a consultant for Roche, Novartis, and Biogen. **FB** is Scientific consultant to Bayer-Schering, Sanofi-Genzyme, Novartis, Biogen, Merck, Roche, Janssen, TEVA, Genzyme, Eisai, Apitope and GeNeuro; he is an Editorial Boards member for Brain, Multiple Sclerosis Journal, Neuroradiology, Radiology, Neurology; he is consultant for Synthon, Janssen, Novartis, Biogen-Idec, Roche, TEVA, Merck, Apitope; he has received funding from EuroPOND co-PI (H2020), AMYPAD coordinator (IMI), NIHR- UCLH biomedical research centre, Dutch foundation for MS Research. **ATT** has received speaker honoraria from Biomedia, Sereno Symposia International

Foundation, Bayer and meeting expenses from Biogen Idec and is the UK PI for two clinical trials sponsored by MEDDAY pharmaceutical company (MD1003 in optic neuropathy [MS-ON] and progressive MS [MS-SPI2]). **MHJH, BK, CHS, DRA, SO and BMT** have nothing to disclose.

**References:**


1. Miller DH, Chard DT, Ciccarelli O. Clinically isolated syndromes. *Lancet Neurol* 2012; 11: 157–69.
2. Enzinger C, Fazekas F. Measuring gray matter and white matter damage in MS: Why this is not enough. *Front Neurol* 2015; 6: 1–4.
3. Tomassini V, Matthews PM, Thompson AJ, et al. Neuroplasticity and functional recovery in multiple sclerosis. *Nat Rev Neurol* 2012; 8: 635–46.
4. Maguire EA, Gadian DG, Johnsrude IS, et al. Navigation-related structural change in the hippocampi of taxi drivers. *Proc Natl Acad Sci U S A* 2000; 97: 4398–403.
5. Golestani N, Paus T, Zatorre RJ. Anatomical correlates of learning novel speech sounds. *Neuron* 2002; 35: 997–1010.
6. Lerch JP, Worsley K, Shaw WP, et al. Mapping anatomical correlations across cerebral cortex (MACACC) using cortical thickness from MRI. *Neuroimage* 2006; 31: 993–1003.
7. Chen ZJ, He Y, Rosa-Neto P, et al. Revealing modular architecture of human brain structural networks by using cortical thickness from MRI. *Cereb Cortex* 2008; 18: 2374–2381.
8. Tijms BM, Seris P, Willshaw DJ, et al. Similarity-based extraction of individual networks from gray matter MRI scans. *Cereb Cortex* 2012; 22: 1530–1541.
9. Bassett DS, Bullmore E, Verchinski BA, et al. Hierarchical Organization of Human Cortical Networks in Health and Schizophrenia. *J Neurosci* 2008; 28: 9239–9248.
10. Tijms BM, Möller C, Vrenken H, et al. Single-Subject Grey Matter Graphs in Alzheimer's Disease. *PLoS One* 2013; 8: 1–9.
11. van Duinkerken E, Ijzerman RG, Klein M, et al. Disrupted subject-specific gray matter network properties and cognitive dysfunction in type 1 diabetes patients with and without proliferative retinopathy. *Hum Brain Mapp* 2016; 37: 1194–1208.
12. He Y, Chen ZJ, Evans AC. Small-world anatomical networks in the human brain revealed by cortical thickness from MRI. *Cereb Cortex* 2007; 17: 2407–2419.

13. Tewarie P, Steenwijk MD, Tijms BM, et al. Disruption of structural and functional networks in long-standing multiple sclerosis. *Hum Brain Mapp* 2014; 35: 5946–5961.
14. Muthuraman M, Fleischer V, Kolber P, et al. Structural brain network characteristics can differentiate CIS from early RRMS. *Front Neurosci* 2016; 10: 1–12.
15. Rimkus CM, Schoonheim MM, Steenwijk MD, et al. Gray matter networks and cognitive impairment in multiple sclerosis. *Mult Scler J*. Epub ahead of print 2018. DOI: 10.1177/1352458517751650.
16. Watts DJ, Strogatz SH. Collective dynamics of 'small-world' networks. *Nature* 1998; 393: 440–442.
17. Hagens MH, Burggraaff J, Kilsdonk ID, et al. Impact of 3 Tesla MRI on interobserver agreement in clinically isolated syndrome: A MAGNIMS multicentre study. *Mult Scler* 2018; 1352458517751647.
18. Hagens MHJ, Burggraaff J, Kilsdonk ID, et al. Three-Tesla MRI does not improve the diagnosis of multiple sclerosis. *Neurology* 2018; 91: e249–e257.
19. Rovira À, Wattjes MP, Tintoré M, et al. Evidence-based guidelines: MAGNIMS consensus guidelines on the use of MRI in multiple sclerosis-clinical implementation in the diagnostic process. *Nat Rev Neurol* 2015; 11: 471–82.
20. Thompson AJ, Banwell BL, Barkhof F, et al. Diagnosis of multiple sclerosis: 2017 revisions of the McDonald criteria. *Lancet Neurol* 2018; 17: 162–173.
21. Sudre CH, Cardoso MJ, Bouvy WH, et al. Bayesian model selection for pathological neuroimaging data applied to white matter lesion segmentation. *IEEE Trans Med Imaging* 2015; 34: 2079–102.
22. Prados F, Cardoso MJ, MacManus D, et al. A modality-agnostic patch-based technique for lesion filling in multiple sclerosis. *Med Image Comput Comput Assist Interv* 2014; 17: 781–8.
23. Cardoso MJ, Modat M, Wolz R, et al. Geodesic Information Flows: Spatially-Variant Graphs

and Their Application to Segmentation and Fusion. *IEEE Trans Med Imaging* 2015; 34: 1976–1988.

24. Klein A, Tourville J. 101 Labeled Brain Images and a Consistent Human Cortical Labeling Protocol. *Front Neurosci* 2012; 6: 171.
25. Kiselev VG, Hahn KR, Auer DP. Is the brain cortex a fractal? *Neuroimage* 2003; 20: 1765–74.
26. Rubinov M, Sporns O. Complex network measures of brain connectivity: Uses and interpretations. *Neuroimage* 2010; 52: 1059–1069.
27. Zuo X-N, Ehmke R, Mennes M, et al. Network Centrality in the Human Functional Connectome. *Cereb Cortex* 2012; 22: 1862–1875.
28. Joyce KE, Laurienti PJ, Burdette JH, et al. A new measure of centrality for brain networks. *PLoS One* 2010; 5: e12200.
29. Bullmore E, Sporns O. Complex brain networks: Graph theoretical analysis of structural and functional systems. *Nat Rev Neurosci* 2009; 10: 186–198.
30. van Wijk BCM, Stam CJ, Daffertshofer A. Comparing brain networks of different size and connectivity density using graph theory. *PLoS One* 2010; 5: e13701.
31. White H. A Heteroskedasticity-Consistent Covariance Matrix Estimator and a Direct Test for Heteroskedasticity. *Econometrica* 1980; 48: 817–838.
32. Huber PJ. The behavior of maximum likelihood estimates under non-standard conditions. In: *Proceedings of the Fifth Berkeley Symposium on Mathematical Statistics and Probability*. University of California Press, Berkeley, 1967, pp. 221–233.
33. Genovese CR, Lazar NA, Nichols T. Thresholding of statistical maps in functional neuroimaging using the false discovery rate. *Neuroimage* 2002; 15: 870–8.
34. Afifi AA, Kotlerman JB, Ettner SL, et al. Methods for improving regression analysis for skewed continuous or counted responses. *Annu Rev Public Health* 2007; 28: 95–111.
35. Tintoré M, Rovira A, Río J, et al. Baseline MRI predicts future attacks and disability in

clinically isolated syndromes. *Neurology* 2006; 67: 968–72.